Passive Focused Monitoring and Non-invasive Irradiation of Head Tissue Phantoms at Microwave Frequencies

Konstantinos T. Karathanasis, Ioannis A. Gouzouasis, Irene S. Karanasiou, *Member IEEE*, George Stratakos, and Nikolaos K. Uzunoglu, *Fellow Member, IEEE*

***Abstract*—In this work, a novel hybrid system able to provide focused microwave radiometric temperature and/or conductivity measurements and hyperthermia treatment via microwave irradiation is experimentally tested. The main module of the system is an ellipsoidal cavity, which provides the appropriate focusing of the electromagnetic energy on the area of interest. The system has been used the past few years in experiments with different configuration setups including phantom, animal and human volunteer measurements yielding promising outcome. New aspects of our research are presented in this paper regarding both radiometry and hyperthermia modules. On one hand, it is examined whether the system is capable of sensing real time progressive local variations of temperature and/or conductivity in customized phantom setups; on the other, the focusing attributes of the system are explored for different positions and types of phantoms used for hyperthermia. The results show that the system is able to detect local concentrated gradual temperature and conductivity variations expressed as an increase of the output radiometric voltage. When contactless focused hyperthermia is performed, the results show significant temperature increase at specific phantom areas. In this case, the effect of a dielectric matching layer placed around the phantoms has been also tested resulting in the enhancement of the energy penetration depth.**

I. Introduction

PASSIVE imaging techniques use only naturally generated signals from the body and are therefore entirely safe for the subject. In this context, a Microwave Radiometry Imaging System (MiRaIS) has been developed in the Microwave and Fiber Optics Laboratory of the National Technical University of Athens [1]-[5]. The operating principle of the system is based on the use of an ellipsoidal conductive wall cavity for beamforming and focusing on the brain areas of interest. One of the biggest advantages of this method is that it operates in an entirely passive and non-invasive manner.

MiRaIS has been used for the past 4 years in various experiments in order to evaluate the system as a potential intracranial imaging device as well as a system for performing and monitoring hyperthermia treatment [6]-[7]. The MiRaIS system is able to provide real-time temperature and/or conductivity variation measurements in water phantoms and animals and potentially in subcutaneous biological tissues. Both spatial resolution and detection depth provided by the system have been estimated through detailed theoretical analysis and validation experimental procedures using phantoms and animals [1],[2],[5]. In the range 1.3-3.5 GHz, imaging of the head model areas placed at the ellipsoid's focus is feasible with a variety of detection/penetration depths (ranging from 2 cm to 4.5 cm) and spatial resolution (ranging from less than 1 cm to over 3 cm), depending on the frequency used. The system's temperature resolution ranges from 0.5 ^{o}C to less than 1 ^{o}C in phantom and small animal experiments.

Importantly, the system has been used in human experiments in order to explore the possibility of passively measuring brain activation changes that are possibly attributed to local conductivity changes. The results indicate the potential value of using focused microwave radiometry to identify brain activations possibly involved or affected in operations induced by particular psychophysiological tasks [1].

As stated above, the MiRaIS system measures temperature and/or conductivity fluctuations at low microwave frequencies. It has been suggested that brain temperature fluctuations reflect neural activation [8]. Although it is known that relatively large increases in local brain temperature may occur during behavioural tasks and in response to various stressful and emotionally arousing environmental stimuli, the source of this increase is not clearly understood. Empirical data obtained with fMRI suggest that increases in regional cerebral blood flow during functional stimulation can cause local changes in brain temperature and subsequent local changes in oxygen metabolism [9].

Nevertheless brain temperature in humans remains generally unknown because of virtually no direct experimental studies. Although it is known that temperature affects multiple chemical and physical processes in the brain and that relatively weak hyperthermia may damage neural cells, many basic questions regarding brain temperature fluctuations and their regulation in normal and pathological conditions remain unanswered [10].

The existence and severance of sideffects and drawbacks

Manuscript received July 5, 2008. This work has been funded by the project PENED 2003(03ED/226). The project is co-financed 80% of public expenditure through EC - European Social Fund, 20% of public expenditure through Ministry of Development - General Secretariat of Research and Technology and through private sector, under measure 8.3 of operational programme "COMPETITIVENESS" in the 3rd Community Support Programme".

K. T. Karathanasis, I. A. Gouzouasis, I. S. Karanasiou and N. K. Uzunoglu are with the National Technical University of Athens, School of Electrical and Computer Engineering, 9 Iroon Politechneiou, Zografou, 15780, Greece.

Corresponding author is I. S. Karanasiou (phone: +302107722289; fax: +302107723557; e-mail: ikaran@esd.ece.ntua.gr).

of brain hyperthermia treatment, such as brain oedema and possible neurotoxicity, remains a controversial issue. Since most of the experiments reported in literature were conducted under anesthesia, it appears that the passive heating of the brain may be an entirely different phenomenon than the stress associated with heating in the conscious state, related to neurotoxicity. Moreover, several anesthetics, e.g., pentobarbital and ketamine are known neuroprotective agents [11]-[12].

Additionally, knowledge of the electrical conductivity properties of excitable tissues is essential for relating the electromagnetic fields generated by the tissue to the underlying neurophysiological mechanisms. The electrical conductivity of the brain is determined by the relative volumes and differing impedances of the neurons, glial cells, blood, and extra-cellular fluid. If changes in the relative volume of these components occur, brain conductivity will be affected. Thus, it has been suggested that an increase of regional cerebral blood volume (rCBV) due to neuronal activity will lead to the decrease of cortical impedance (increase of conductivity) because blood has lower impedance than the surrounding cortex [13]. During functional activity, there is a predominant impedance decrease as a result of an increase in blood volume. Since brain activation produces changes in regional cerebral blood flow (rCBF), it will also produce conductivity changes in the same direction. These (increased usually) blood-flow changes are associated to increased rCBV. Also, recently, reproducible impedance changes of approximately 0.5% were measured in humans during visual or motor activity, using 3-D electrical impedance tomography (EIT) [14].

Following this rationale, if such changes can be measured with the proposed method, then it could be used to image brain activity in an entirely passive and non-invasive manner that it is completely harmless and can be repeated as often as necessary without any risk even for sensitive populations such as children and pregnant women.

Microwave radiometry monitoring is well known for more than 30 years; however, we have implemented it following totally innovative approaches (i.e., contactless remote monitoring while most existing systems were radiometry near-field applications) in order to achieve completely passive functional imaging, hyperthermia treatment and monitoring during the latter. Therefore, focused Microwave Radiometry, used in the past only for in depth body temperature monitoring, is proposed herein for 1) totally passive functional brain imaging and 2) for performing non-invasive intracranial hyperthermia treatment and monitoring.

New aspects of our research are presented in this paper regarding both radiometry and hyperthermia modules. On one hand, it is examined whether the system is capable of sensing real time gradual local variations of temperature and/or conductivity in customized phantom setups; on the other, the focusing attributes of the system are explored for different positions and types of phantoms used for hyperthermia.

II. Materials and Methods

A. System description

The novel system presented in this work is investigated as a device to provide focused radiometry measurements and hyperthermia treatment at microwave frequencies. Its main module is an ellipsoidal conductive wall cavity, providing the necessary focusing of the electromagnetic energy on the area of interest. The geometrical properties of the ellipse indicate that rays, emitted from one focal point, will merge coherently on the other focal point. Exploiting this characteristic, when the system is used for microwave radiometry the medium of interest is placed at one focal point, whereas a receiving antenna is placed at the other one. In this way, the chaotic electromagnetic energy emitted by the medium is received by the antenna and driven to a radiometer for detection (Fig. 1). On the other hand, when hyperthermia is performed, the receiving antenna is replaced by an emitting one. In this case, the emitted electromagnetic energy is focused on a certain area of the medium of interest, depending on its position in respect to the focal point (Fig. 1).

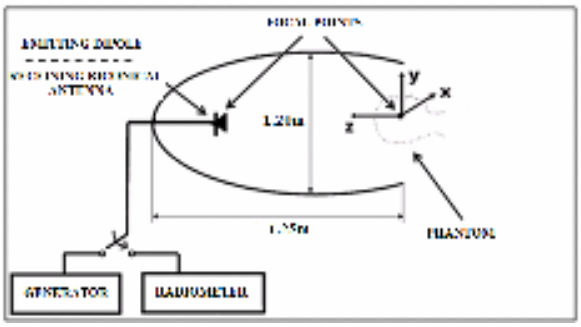

Fig. 1. Block diagram of the hybrid system. All the main modules, implementing its dual use, are illustrated.

Apart from the ellipsoidal cavity, the remaining main parts of the system comprise a biconical antenna in conjunction with a receiver, used in radiometry measurements, and a generator connected to a dipole antenna, used in hyperthermia.

The constructed multiband radiometer (Fig. 2a) is based on the parallel processing concept. Parallel processing requires that the spectrum has been split in four sub-bands 1.1 GHz, 1.8 GHz, 2.4 GHz and 2.8 GHz each one with approximately 150 MHz bandwidth. For each band a dedicated logarithmic detector is used which gives the capability of power sensing down to -110dBm. The whole system which comprises the four sub-systems is fed by a low noise amplifier which has a gain of approximately 35dB and a noise figure less than 2 dB in the band of interest (1-3 GHz). The low noise amplifier output is split in four outputs in order to fit the four radiometer sub-systems. The logarithmic detection part on each radiometer sub-system is exactly the same and it is followed by a buffer-amplifier stage. In order to avoid EMI/EMC problems each radiometer

sub-system is housed into highly sealed aluminum boxes. Power supply to the system is +/-12VDC. The radiometer is connected to a broadband biconical antenna, having very low returning losses in the range of 1-3GHz (Fig. 2b).

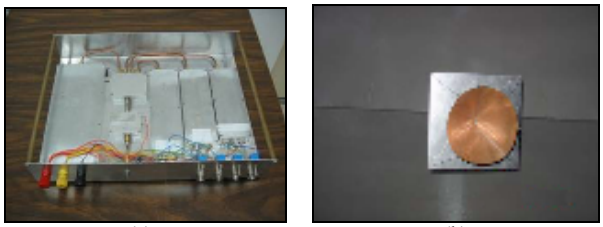

(a) (b)

Fig. 2. Photograph of the multiband radiometer and the broadband biconical antenna used in the radiometry experiments.

According to previous theoretical studies ([1], [3]) the measured voltage at the output of the radiometer is proportional to

$$I = \left(\omega_0^2 \mu_o k / \pi\right) \Delta\omega \iiint_V \Gamma_A\left(\bar{r}'\right) T\left(\bar{r}'\right) \sigma\left(\bar{r}'\right) d\bar{r}' \quad (1)$$

where, k is the Boltzman's constant, ω_0 is the centre frequency (in radians/sec) of the bandwidth of the observed microwave spectrum, μ_0 is the free space magnetic permeability, V is the volume of the focusing area, $T\left(\bar{r}'\right)$ is the temperature spatial distribution within the medium of interest, $\sigma\left(\bar{r}'\right)$ is the spatial distribution within the medium of interest for the electric conductivity and $\Gamma_A\left(\bar{r}'\right)$ is the Kernel function related to the observed medium Green's function, taking into account the electromagnetic properties of the receiving antenna.

The hyperthermia module comprises a magnetron generator operating at 2.45 GHz (Fig. 3) in conjunction with the ellipsoidal reflector. The electromagnetic energy is fed to a matching dipole antenna and gel saline phantoms are placed on the opposite focal point receiving the emitted electromagnetic waves.

B. Experiments

Experiments that were conducted in previous studies investigated the system's ability to detect phantoms of constant conductivity but being at different temperatures [1]-[5]. The results showed that the system was able to provide different output for the various phantom temperatures. In this paper, the temperature of only a partial volume of the phantom is gradually changed and detected by the system in real-time. Similar experiments were performed for local progressive phantom conductivity changes. The phantoms used were de-ionized and aqua based and the conductivity variations were performed using saline solutions.

During the hyperthermia experiments, different positions of the phantom in respect to the focal point are investigated and each time the energy absorbing areas are observed. The experimental procedure also included the use of a dielectric matching layer placed around the phantom. The use of dielectric materials as intermediary layers between the air and the medium of interest, creates a stepped change of the refraction index on this interface and thus, reduces the scattering effects of the electromagnetic energy, as previous theoretical studies have shown [15],[16].

Fig. 3. Photograph of the 2.45GHz generator used in the hyperthermia experiments.

III. RESULTS

A. Focused microwave radiometry experiments

In this section the results of the microwave radiometry measurements are presented. The experimental setup is depicted in figure 4. The experiments were performed in order to validate that the system is able to detect both temperature and conductivity variations as previously mentioned. Since the hyperthermia module operates at 2.45GHz, we present the radiometric measurement results at the same frequency for consistency and to enable comparison of the findings. All the experimentation was carried out in an anechoic Faraday chamber.

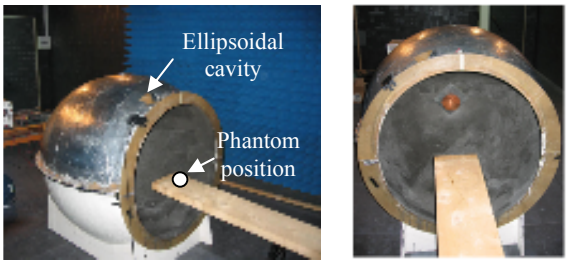

(a) (b)

Fig. 4. a) Photograph of the setup used for the microwave radiometry measurements. b) The biconical antenna placed at the one focal point in the inside of the ellipsoidal.

For the temperature experimentation, the setup involved the use of two cylindrical containers; one with 7cm radius and 6cm height and a smaller one with 2cm radius and equal height. The large container was filled with de-ionized water at room temperature, whereas the small one was gradually filled with tepid de-ionized water during the experiments. For the conductivity experimentation, the same large container was filled with de-ionized water based gel,

containing one spherical area of 3cm diameter which during the procedure was filled with a saline water solution in the same temperature.

The experimental procedure for the temperature measurements was as follows (Fig. 5): Until time point t=50s the radiometer measured just the background noise (baseline). At that moment the large container was placed in the system, centered at the focal point (*phase I*). At t=80s the smaller container placed at the focal point was filled with tepid water (*phase II*). At t=110s the small container was misplaced by 2 cm away from the focal point (*phase III*) until t=140s, when it was centered again exactly at the focal point (*phase IV*) and stayed till t=170s when it was totally removed (*phase V*). Finally, at t=200s the large container was also removed.

In Fig. 5a the radiometric output at 2.45GHz is presented. It is obvious that the radiometer detected the five separate phases of the experiment. As the experiment evolves it is concluded that the system can successfully detect local changes of temperature in a cool environment with spatial sensitivity of at least 2cm.

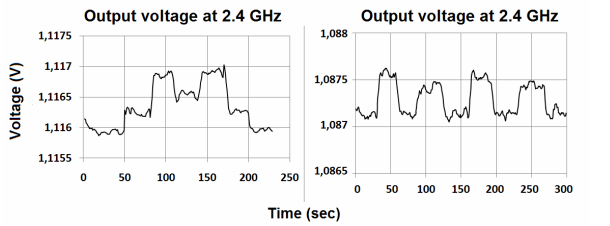

(a) (b)

Fig. 5. Radiometric output for the (a) temperature and (b) conductivity measurements.

In this paragraph the procedure followed for the conductivity measurements is presented. Until time point t=30s the de-ionized water-based gel phantom was inserted in the system with the geometrical center of the small hemispherical area placed at the focal point of the ellipsoidal. At point t=30s, the saline water solution (having the same temperature as the gel) was placed inside the hemispherical area (*phase I*) where it remained for 30 seconds until it was removed. At time point t=90s the spherical area of 3cm diameter was filled with de-ionized water (at the same temperature as the gel) again for 30 seconds (*phase II*). This was done in order to make sure that the change in the radiometer's output observed in *phase I* was not only due to the increase in the volume of the phantom (eq. 1), but also due to the different conductivity value of the spherical area. These two steps were repeated twice in order to check repeatability of the system's response.

In fig. 5b the radiometric output at 2.45GHz is once again depicted. It is concluded that the system is able to detect local conductivity variations as in phases I and II the voltage output is at different levels. More specifically, the same volumes changes of de-ionized water and saline water solutions, having the same temperature, produce different variations on the radiometer's output voltage.

B. Hyperthermia experiments

The hyperthermia experiments were performed in order to investigate the system's focusing properties at the frequency of 2.45GHz. More specifically, the system's spatial sensitivity was tested using saline water gel phantoms that were placed at several positions in respect to the ellipsoid's focal point. Another aspect concerning the system's focusing properties is the use of a dielectric matching layer placed around the gel phantom. For this reason, a second experimentation included the placement of a low loss dielectric layer around the phantom prior to the irradiation and the effect on the energy absorbing areas was observed.

During both hyperthermia experiments, the same container was used as in the radiometry measurements. In this case however, the container was filled with saline water based gel at 9^{o}C (Fig. 6). The matching layer was lossless with dielectric permittivity value of ε_r=6 and thickness 1.5 cm. The generator was adjusted to operate at 200 Watts for 200 seconds duration.

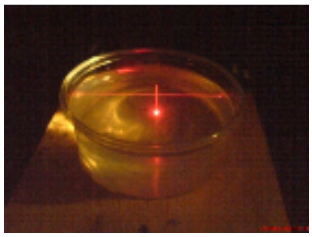

Fig. 6. The saline water based gel used for the hyperthermia experiments. Three laser beams accurately indicate the position of the focal point.

During the hyperthermia experiments two different phantom areas were placed at the ellipsoidal focal area and irradiation was performed with and without use of dielectric matching material.

In the first case, the container was placed with its geometrical center on the focal point of the ellipsoidal. After the irradiation, the temperature distribution on the container's surface was measured. As figure 7 shows, there were two small areas on the edge of the container that were particularly heated. These two areas coincide with the direction of propagation of the electromagnetic wave, as it is theoretically calculated [15], [16] and an important temperature increase of about 10^{o}C was observed as deep to 1cm from the edge of the container. Also, it is shown that the penetration depth of the electromagnetic energy at 2.45GHz is 2-3 cm inside the water based phantom, as it can be assumed that the temperature rise till this depth was due to the irradiation and not to the heat diffusion inside the phantom. Furthermore, a circular area of 3cm radius around the focal point seemed to be unaffected by the irradiation. Finally, an area of small depth ($\approx$ 0.5 cm) was heated around

the outer perimeter of the phantom.

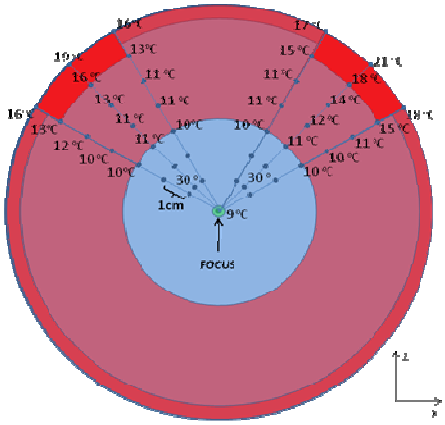

Fig. 7. Temperature distribution projected on the surface of the gel phantom after irradiation. The center of the phantom is placed on the ellipsoidal's focal point.

In the next case, the dielectric matching layer is placed around the phantom. Again the center of the phantom is placed at the focal point. Figure 8 shows the temperature distribution projected on the phantom's surface. Once again, the same areas as in figure 7 were heated, but in this case the temperature increase was greater and observed at a larger depth (15-18^{o}C for 2-3cm deep). Also, the highest temperature observed was 27^{o}C, indicating an increase of 18^{o}C from the initial surface temperature. These findings indicate that the use of the dielectric matching layer results in the reduction of the reflected electromagnetic energy on the air-phantom interface and consequently to the higher penetration of the energy in the phantom's interior, verifying previous theoretical findings.

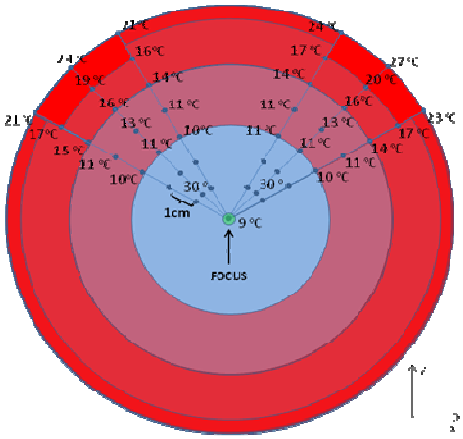

Fig. 8. Temperature distribution projected on the surface of the gel phantom after irradiation. The center of the phantom is placed on the ellipsoidal's focal point. The dielectric matching layer is placed around the phantom.

The second experimental procedure involved the investigation of the system's focusing properties when an arbitrary area is placed at the focal area. In this case, the focal point was 4cm far from the container's center along the 'x' axis and 4cm along the 'z' axis. As shown in figure 9, the placement of the focal point close to the edge of the container caused the widening of the frontal heated area, whereas the second area remained unchanged. In overall, the temperature pattern seemed almost identical to the two previous cases, indicating the highest increase of 13^{o}C at the outer edge of the container.

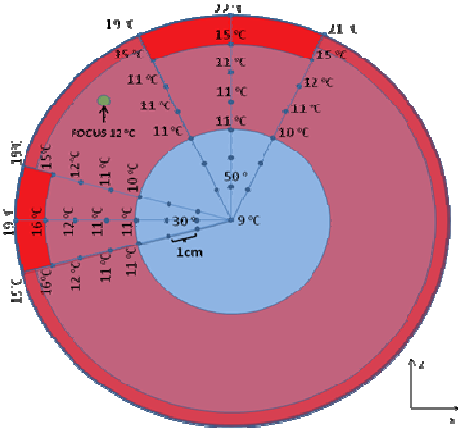

Fig. 9. Temperature distribution projected on the surface of the gel phantom after irradiation. The center of the phantom is 4cm far from the focal point in the 'x' axis and 4cm from the 'z' axis.

Finally, in the last experiment procedure the layer of the dielectric material was again placed around the phantom. The resulting temperature distribution is illustrated in figure 10, where, as expected, the temperature values are higher than those in figure 9. The energy has been absorbed in different quantities till the depth of 4cm from the container's edge and again the highest temperature was recorded at the frontal edge of the container.

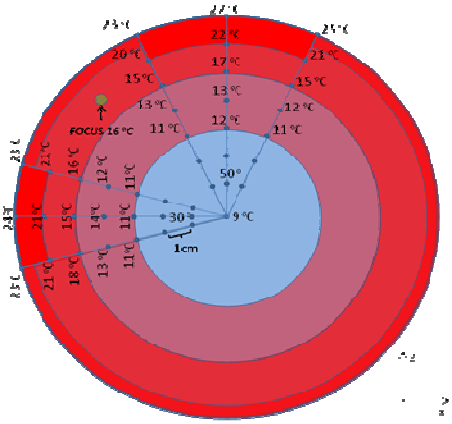

Fig. 10. Temperature distribution projected on the surface of the gel phantom after irradiation. The center of the phantom is 4cm far from the focal point in the 'x' axis and 4cm from the 'z' axis. The dielectric matching layer is placed around the phantom.

IV. Discussion and Conclusion

In this paper, a novel hybrid system was experimentally tested in order to initially investigate the ability of providing real-time measurements of local temperature and/or conductivity variations on different phantom setups. The experiments, implementing the focused microwave radiometry technique, revealed such a potential by detecting the local concentrated gradual temperature and conductivity variations expressed as an increase of the output radiometric voltage. More specifically, water phantoms with small volume areas of different temperatures or having different local conductivity values produced different output radiometric voltage.

Another aspect investigated through the present work was the focusing properties of the system, when focused hyperthermia is performed. Aqua based phantoms were used for this reason and were irradiated at 2.45GHz at several positions in respect to the ellipsoidal's focal point. The results showed significant temperature increase at specific phantom areas revealing the main energy-absorbing areas of the corresponding frequency. Also, in this case, the effect of a dielectric matching layer placed around the phantoms was tested, resulting in the enhancement of the energy penetration depth.

By providing estimations of intracranial temperature in an entirely passive manner, the scope of our research efforts is to possibly add to the knowledge on the influence of brain temperature as a parameter that provides information on normal brain functions and the development of brain pathology. The way that brain temperature fluctuates under normal physiological and behavioral conditions may elucidate the mechanisms underlying these fluctuations. A fluctuation in brain temperature within 4°C may be considered as normal physiological response [17]. It is not known yet whether the fluctuations found in animal experiments occur in the human brain but, based on similarities found between rats and monkeys [18], it appears likely.

Since similar to neuronal discharges brain temperatures and conductivities are affected by various salient sensory stimuli and drugs, show consistent changes during learning, and fluctuate during motivated behavior, tightly correlating with key behavioral events, the proposed system may add to the clarification of the relationships between these underlying parameters in the future.

Deep brain hyperthermia treatment appears to be promising against brain cancerous tumors in conjunction with other cancer treatments. Temperature monitoring during hyperthermia is a crucial factor for successful treatment and the proposed system attempts to provide both and in a total non-invasive contactless way. Future experiments will focus on improving the spatial selectivity and volume size of the heating areas by performing irradiation also at lower microwave frequencies which will enable larger penetration depths.

V. Acknowledgment

This research project is co-financed by E.U.-European Social Fund (80%) and the Greek Ministry of Development-GSRT (20%).

References

[1] I. S. Karanasiou, N. K. Uzunoglu and C. Papageorgiou, "Towards functional non-invasive imaging of excitable tissues inside the human body using Focused Microwave Radiometry", *IEEE Trans. Microwave Theory Tech.*, vol. 52, no. 8, pp. 1898-1908, Aug. 2004.

[2] I. S. Karanasiou, and N. K. Uzunoglu, "Experimental Study of 3D Contactless Conductivity Detection using Microwave Radiometry: a Possible Method for Investigation of Brain Conductivity Fluctuations", *Proceedings of the 26th IEEE EMBS*, pp. 2303-2306, 2004.

[3] I. S. Karanasiou, N. K. Uzunoglu, S. Stergiopoulos, and W. Wong, "A Passive 3D Imaging Thermograph Using Microwave Radiometry", *Innovation and Technology in Biology and Medicine*, vol. 25 (4), pp. 227-239, 2004.

[4] I. S. Karanasiou, and N. K. Uzunoglu, "The Inverse Problem of a Passive Multiband Microwave Intracranial Imaging Method", *Proceedings of the 27th IEEE EMBS*, 2005.

[5] I. S. Karanasiou, and N. K. Uzunoglu, "Single-frequency and Multiband Microwave Radiometry for Feasible Brain Conductivity Variation Imaging during Reactions to External Stimuli", *NIMA J.,* vol. 569, pp. 581-586, 2006.

[6] I. S. Karanasiou, and N. K. Uzunoglu, "Study of a Brain Hyperthermia System providing also Passive Brain Temperature Monitoring", *Proceedings of the 28th IEEE EMBS,* pp. 5017-5020, 2006.

[7] I. S. Karanasiou, K. T. Karathanasis, A. Garetsos, and N. K. Uzunoglu, "Development and Laboratory Testing of a Non-invasive Intracranial Focused Hyperthermia System", *IEEE Trans. Microwave Theory Tech (under publication).*

[8] E. A. Kiyatkin, P. L. Brown, and R. A. Wise, "Brain temperature fluctuation: a reflection of functional neural activation", *Europ. J. Neuroscience,* vol. 16, pp. 164-168, 2002.

[9] D. A. Yablonskiy, J. H. Ackerman, and M. E. Raichle, "Coupling between changes in human brain temperature and oxidative metabolism during prolonged visual stimulation", *Proc. Nat. Acad. Sci.,* vol. 97, pp. 7603-7608, 2000.

[10] E. A. Kiyatkin, "Brain temperature fluctuations during physiological and pathological conditions", *Europ. J. Appl. Physiol.,* vol. 101, pp. 3-17, 2007.

[11] S. K. Salzman, *Neural monitoring. The prevention of intraoperative injury*, New Jersey: Humanna Press, 1990.

[12] H. S. Sharma, "Hyperthermia induced brain oedema: Current status & future perspectives", *Indian J. Med. Research*, May 2006.

[13] L. A. Geddes, and L. E. Baker, "The specific resistance of biological material: A compendium of data for the biomedical engineer and physiologist", *Med. Bio. Eng.,* vol. 5, pp 271-293, 1967.

[14] T. Tidswell, A. Gibson, R. H. Bayford, and D. S. Holder, "Thee-dimensional electrical impedance tomography of human brain activity", *Neuroimage*, vol. 13, pp. 283-294, 2001.

[15] K. T. Karathanasis, I. S. Karanasiou, and N. K. Uzunoglu, "A FEM Simulation Study of the Optimization of the Imaging Attributes of a Microwave Radiometry System with Possible Functional Imaging Capabilities", *NIMA J. (under publication)*, 2007.

[16] I. A. Gouzouasis, I. S. Karanasiou, and N. K. Uzunoglu, "Exploring the Enhancement of the Imaging Properties of a Microwave Radiometry System for Possible Functional Imaging Using a Realistic Human Head Model", *NIMA J. (under publication),* 2007.

[17] E. A. Kiyatkin, "Brain hyperthermia as physiological and pathological phenomena", *Brain. Res. Rev.*, vol. 50, pp. 27-56, 2005.

[18] J. N. Hayward, and M. A. Baker, "Role of cerebral arterial blood in the regulation of brain temperature in the monkey", *Am. J. Physiol.*, vol. 215, pp. 389–403, 1968.